EphA2-mediatedM1-like polarization of microglia attenuatesglioblastoma metastasis

Xiang Liao (liaoxiang025@126.com)
Nanjing Jinling Hospital

Ru Fang
Jinling Hospital

Ying Tian
Nanjing Jinling Hospital: East Region Military Command General Hospital

Chen Chen
Changzhou First People's Hospital

Zhijun Wu
Southeast University Zhongda Hospital

Jing Sun
Nanjing Jinling Hospital: East Region Military Command General Hospital

Jianrui Li
Nanjing Jinling Hospital: East Region Military Command General Hospital

Xiaoxue Liu
Nanjing Jinling Hospital: East Region Military Command General Hospital

Ming Li
Ma'anshan People's Hospital

Guangming Lu
Nanjing Jinling Hospital: East Region Military Command General Hospital

Research

Keywords: Glioblastomamultiforme, EphA2,miroglia,polarization

Posted Date: October 8th, 2020

DOI: https://doi.org/10.21203/rs.3.rs-86074/v1

Abstract

Background

EphA2 is upregulated in GBM tumor tissue specimens and established cancer cell lines and thought to be an attractive therapeutic target in cancer. We aim to define the role of EphA2 in polarization of microglia.

Methods

Quantitative real-time polymerase chain reaction, immunofluorescence staining, and viral transfection-based knockdown and overexpression assays to assess the effect of EphA2 on microglia polarization. iTRAQ-LC-MS/MS and western blot were conducted to detect EphA2 and PI3K-Akt signaling activity. Using the Millicell system as an *in vitro* co-culture model, we performed transwell and western blot assays investigate the role of EphA2-mediated M1-like of microglia on GBM cells invasion and migration *in vitro* and *in vivo*.

Results

In overexpressing and silencing experiments, we demonstrated that EphA2 contributed to the M1-like polarization of microglia. Mechanistically, PI3K-AKT signaling was the downstream of EphA2 and supported the process of EphA2 mediated the M1-like polarization of microglia. Finally, EphA2 mediated the M1-like polarization of microglia attenuated the migration and invasion ability of GBM cells *in vitro* and *in vivo*.

Conclusions

Our study indicates that, distinct from its role on cancer cells, EphA2 promoted the M1-like polarization of microglia and further attenuated the metastasis of GBM.Our results provide a new information on rationale for targeting EphA2 to improve treatment outcomes in GBM patients.

Background

Glioblastoma multiforme (GBM) is the most common and lethal malignant primary brain tumor, with the characteristic of highly invasion and recurrence[1, 2]. Due to the tumor cell and genetic heterogeneity, GBM patients respond minimally to current therapies, including surgery, radiation and chemotherapy. In addition to eradicating cancer cells, remolding non-cancerous stromal cells in the tumor microenvironment represent a promise alternative therapeutic avenues.

As the richest and critical components in the tumor microenvironment, tumor-associated macrophages (TAMs) are significant correlation with GBM patient prognosis, progression and grades[3]. Crosstalk between cancer cell and TAM is critical for invasion and recurrence of GBM. TAMs have two extremes of the phenotypic spectrum, which are defined as the alternatively activated protumor (M2) versus classically activated antitumor (M1) states[4]. Notably, inducing TAM polarization into the M1-like

subtype has been reported to block GBM progression[5, 6]. Despite the convincing functional of M1-like macrophage, the precise mechanisms for the polarization of TAM to M1-like subtype remain largely unclear.

As the most important class of receptor tyrosine kinases, Ephrin(Eph) kinases family attract increasing attention in carcinogenesis and tumor progression[7]. Different from the majority of Eph kinases that are mostly synthesized during the developmental process, EphA2 is mainly restricted to proliferating epithelial cells in adults and expressed high level on in human tumor tissue specimens and established cancer cell lines[8, 9]. Recently, more and more researches confirmed that EphA2 expression in cancer cell highly associated with poor prognosis and reduced survival of tumor patients[10, 11]. EphA2 overexpression in epithelial cells can promote oncogenic transformation[12]. As a direct transcriptional target of Ras-Raf-ERK signaling, EphA2 is overexpressed in Ras-transformed cells and prompted breast cancer progression[13]. EphA2 regulates glioblastoma cell proliferation via the MEK/ERK/RSK pathway[14]. Under normal conditions, by binding several receptors, EphA2 could also induce diverse signaling networks in the neighbor cell and following cell-to-cell contact[15]. However, the exact role of EphA2 in microglia polarization and the underlying molecular mechanism remains unclear. Therefore, we are interested if EphA2 induced the M1-like polarization of microglia and further inhibit the metastasis of GBM.

To test this hypothesis, we used the overexpressing and silencing methods and the results suggested that EphA2 induced the M1-like polarization of microglia and PI3K/ AKT signaling axis was involved in the process. Finally, we shown that EphA2 induced the M1-like polarization of microglia attenuated the migration and invasion of GBM cells *in vitro* and *in vivo*. Taken together, our findings demonstrate that, distinct from its role in cancer cells, EphA2 expressed in microglia is a negative regulator of GBM progression.

Materials And Methods

Cell culture and treatment

C6 cells were maintained in Dulbecco's modified Eagle's medium (DMEM) supplied with 10% fetal bovine serum (FBS) and 1% antibiotics. GL261 and BV2 cells were cultured in high glucose DMEM medium with 10% FBS and 1% antibiotics. All cells were incubated in 5% CO_2 at 37 °C. To inhibit or activate PI3K-AKT pathway, cells were treated by Honokiol (HY-N0003, MCE, China) or sc-79 (GC11645, Glpbio, USA) for 24 h.

TCGA analysis

The gene expression of glioma patients in TCGA (The Cancer Genome Atlas) were downloaded by Cancer Brower site (https://xenabrowser.net/datapages/), and the correlation between CD80 and MMP9, BIRC5, MYC and EphA2 was analyzed. High and low groups were defined as above and below the mean respectively

RNA isolation and quantitative real-time PCR (qPCR)

Total RNA was isolated from cells with Total RNA Extraction Reagent (R401-01, Vazyme, Nanjing) according to the manufacturer's instructions. One microgram of RNA was reverse transcribed to cDNA with Hiscript Q RT SuperMix for qPCR (R122-01, Vazyme, Nanjing) as described by the manufacturer's instructions. Quantitative real-time PCR was performed using ChamQ SYBR Master Mix (Q311-02, Vazyme, Nanjing) and a LightCycler 96 (Roche, Risch-Rotkreuz, Switzerland) with the following conditions: 5 min at 95 °C, followed by 40 cycles at 95 °C for 30 s, 60 °C for 40 s and 72 °C for 60 s. All primers used for qPCR are shown in Table 1.

Cell transfection

Adenovirus was used to overexpress mouse EphA2 (Ad-EphA2) packaged by Vigene Biosciences Co., Ltd., (Shandong, China). Lentivirus was used to knockdown mouse EphA2 (LV-siEphA2) and overexpress rat EphA2 (OE-EphA2) packaged by Genechem Co., Ltd., (Shanghai, China). BV2 cells were transfected with Ad-EphA2 and LV-siEphA2. The rat primary microglia was transfected OE-EphA2. The infection results were verified by qPCR and Western blot analysis.

Western blot analysis

Samples (cells) were lysed in RIPA lysis buffer with PMSF and a protease/phosphatase inhibitor (Cell Signaling Technology, USA). A total of 30 μg of protein per sample was loaded onto an SDS-PAGE gel and then transferred onto a 0.22 μm polyvinylidenedifluoride (PVDF) membrane (Merck-Millipore, Germany). The membranes were blocked in PBST with 5% BSA for 1 h at RT and then incubated with primary antibodies at 4 °C overnight, followed by incubation with an HRP-conjugated secondary antibody for 1 h at RT. The membranes were visualized with electrochemiluminescence (ECL) Western Blotting Substrate (Tanon, Shanghai, China) and a Tanon 5200 system (Tanon, Shanghai, China). In our study, the primary antibodies included anti-EphA2, AKT, p-AKT, PI3K, p-PI3K, NLRP3, TNF-α, iNOS, IL-1β, β-catenin, ZEB1, survivin, c-myc(1:1000, Cell Signaling Technology, USA), and β-actin (1:5000, Cell Signaling Technology, USA).

Immunohistochemistry

Tissues were fixed in formalin, dehydrated with alcohol, and paraffin-embedded. Five-micron sections of tissues were cut and stained with eosin and hematoxylin. For IHC staining, 5 μm sections of tissues were stained with antibodies at 4 °C overnight, followed by incubation with HRP-labeled secondary antibodies for 1 h at RT and visualization with a DAB Substrate Kit (Cell Signaling Technology, USA).

Isolation of microglia from neonatal rat

Microglia of neonatal rat were prepared as described elsewhere[16]. Briefly, brains of neonatal SD rat were dissected and dissociated. The cells were seeded in DMEM-F12 medium containing 10% FBS with 75 cm^2 culture flask. On the 14th day, flask was agitated on rotary shaker at 240 rpm for 3 h at 37℃. Collected microglia from the supernatant and suspended the pellet after centrifugation.

Transwell assay

Tumor cell migration and invasion were analyzed by Transwell assays without or with Matrigel. Briefly, 10^4 C6 or GL261 cells were seeded in the upper chamber of a 24-well Transwell or Matrigel chamber with 8 μm pores (Corning Inc., Corning, NY, USA) and serum-free medium. The bottom chamber contained complete medium with 10% FBS and 10^4 BV2-Ad-con or BV2-Ad-EphA2. Following incubation for 24 h or 36 h, the cells on the upper membrane surface were removed with cotton swabs, and cells that migrated or invaded through the filter were fixed with 4% paraformaldehyde for 15 min and stained with 0.5% crystal violet for 5 min. The number of migrated or invaded cells was calculated in 6 randomly selected fields, and each condition was analyzed in triplicate.

Protein digestion and iTRAQ labeling

Protein digestion was performed according to the FASP procedure described in Wisniewski, et al. [17], and the resulting peptide mixture was labeled with the 4-plex/8-plex iTRAQ reagent according to the manufacturer's instructions (Applied Biosystems). Briefly, 200 μg of protein for each sample was mixed with30 μl of STD buffer (4% SDS, 100 mM DTT, 150 mM Tris-HCl pH 8.0). The detergent, DTT and other low-molecular-weight components were removed using UA buffer (8 M urea, 150 mM Tris-HCl pH8.0) and repeated ultrafiltration (Microcon units, 30 kD). Then, 100 μl of 0.05 M iodoacetamide in UA buffer was added to block reduced cysteine residues, and the samples were incubated for 20 min in the dark. The filters were washed with 100 μl of UA buffer three times and then with 100 μl of DS buffer (50 mM ammonium bicarbonate at pH 8.5) twice. Finally, the protein suspensions were digested with 2 μg of trypsin in 40 μl of DS buffer overnight at 37 °C, and the resulting peptides were collected as the filtrate. The peptide content was estimated by UV light spectral density at 280 nm using an extinction coefficient of 1.1 for a 0.1% (g/l) solution calculated on the basis of the frequency of tryptophan and tyrosine in vertebrate proteins.

For labeling, each iTRAQ reagent was dissolved in 70 μl of ethanol and added to the respective peptide mixture. The samples were labeled as (Sample1)-114, (Sample2)-115, (Sample3)-116, and (Sample4)-117 and then multiplexed and vacuum dried.

Enrichment of phosphorylated peptides by TiO2 beads

Labeled peptides were mixed, concentrated with a vacuum concentrator and resuspended in 500 μl of loading buffer (2% glutamic acid/65% ACN/2% TFA). Then, TiO2 beads were added and agitated for 40 min. Centrifugation was performed for 1 min at 5000 g, resulting in the first beads. The supernatant from the first centrifugation was mixed with additional TiO2 beads, resulting in the second beads, which were collected as before. Both beads were combined and washed with 50 μL of wash buffer I (30% ACN/3% TFA) three times and then with 50 μL of wash buffer II (80% ACN/0.3% TFA) three times to remove the remaining non-adsorbed material. Finally, the phosphopeptides were eluted with 50 μL of elution buffer (40% ACN/15% NH4OH)[18], followed by lyophilization and MS analysis.

Mass spectrometry

Five microliters of phosphopeptide solution was mixed with 15 μl of 0.1% (v/v) trifluoroacetic acid, and 10 μl of the solution mixture was then injected for nanoLC-MS/MS analysis using a Q Exactive MS (Thermo Scientific) equipped with Easy nLC (ProxeonBiosystems, now Thermo Scientific). The peptide mixture was loaded onto a C18 reversed-phase column (15 cm long, 75 μm inner diameter, RP-C18 3 μm, packed in-house) with buffer A (0.1% formic acid) and separated with a linear gradient of buffer B (80% acetonitrile and 0.1% formic acid) at a flow rate of 250 nl/min controlled by IntelliFlow technology over 240 min. The peptides were eluted with a gradient of 0–60% buffer B from 0 min to 200 min, 60–100% buffer B from 200 min to 216 min, and 100% buffer B from 216 min to 240 min.

For MS analysis, peptides were analyzed in positive ion mode. MS spectra were acquired using a data-dependent top10 method dynamically choosing the most abundant precursor ions from the survey scan (300–1800 m/z) for HCD fragmentation. Determination of the target value was based on predictive automatic gain control (pAGC). The dynamic exclusion duration was 40.0 s. Survey scans were acquired at a resolution of 70,000 at m/z 200, and the resolution for the HCD spectra was set to 17,500 at m/z 200. The normalized collision energy was 27 eV, and the underfill ratio, which specifies the minimum percentage of the target value likely to be reached at the maximum fill time, was defined as 0.1%. The instrument was run with peptide recognition mode enabled.

Data analysis

MS/MS spectra were searched using Mascot 2.2 (Matrix Science) embedded in Proteome Discoverer 1.4against the Uniprot_mouse database (73952 sequences, downloaded March 18th, 2013) and the decoy database. For protein identification, the following options were used: peptide mass tolerance = 20 ppm, MS/MS tolerance = 0.1 Da, enzyme = trypsin, missed cleavage = 2, fixed modification: carbamidomethyl (C), iTRAQ4-/8-plex(K), iTRAQ4-/8-plex(N-term), and variable modification: oxidation(M), phosphorylation (S/T/Y). The score threshold for peptide identification was set at a 1% false discovery rate (FDR) and a phosphoRS site probability cutoff of 0.75[19].

Stereotactic implantation of glioma cells

Rats were isoflurane-anesthetized and placed in a stereotaxic instrument (Anhui Zhenghua Co., LT., Huaibei, China). The stereotaxic coordinates of the intracranial injection were AP = + 1.6 mm to the bregma, ML = − 2 mm lateral to the bregma, and DV = − 6 mm ventral. The animals received a single microinjection of 1 × 106 C6 rat glioma cells (total 10 μl) or DMEM (10 μl) into the right stratum using a 25 μl syringe (Gaoge, Shanghai, China). The rats were sacrificed on day 14 after injection. The procedures were approved by Ethical Committee for Experiments on Animals of Nanjing University.

Subcutaneous model

C6 (1×10^6) co-cultured with BV2-Ad-con or BV2-Ad-EphA2 for 24 h were injected subcutaneously into 6–8 w nude mice. Tumor size was measured from the third day with caliper after injection and tumor volumes were calculated with $V = \text{length} \times \text{wide}^2/2$. The procedures were approved by Ethical Committee for Experiments on Animals of Nanjing University.

Pulmonary Metastasis Model

Male nude mice (6–8 weeks old) obtained from Model Animal Research Center of Nanjing University. C6 cells were co-cultured with BV2-Ad-con or BV2-Ad-EphA2 for 24 h and then injected into nude mice from tail vein. After 7 days, HE staining was performed to confirm the development of the metastases foci in lungs. The procedures were approved by Ethical Committee for Experiments on Animals of Nanjing University.

Patient samples collection

Tissue specimens and blood samples from glioma patients were obtained from the General Hospital of Eastern Military Command and the First Hospital of Changzhou. The study was approved by the Ethics Committee of Jinling Hospital. For our study, informed consent was signed by all patients. Information of patients was list in the Table 2.

Statistical analysis

All experiments were performed at least three times, and GraphPad Prism 5 was used for statistical analysis. Statistical significance was determined by Student's t-test. P value $\leq .05$ was considered significant.

Results

M1-like polarization of microglia negatively correlation with GBM progression

To investigate the role of microglia polarization in GBM progression, we firstly assessed the M1-like and M2-like microglia related markers expression in GBM orthotopic tumor tissue. The expression level of CD80, M1-like microglia marker, was lower in the tumor tissues than the normal brain tissues, while the expression level of CD206, M2-like microglia marker was *in verse* as shown immunohistochemistry staining (Fig. 1A).

To connect this results to clinical application, using the GBM patient tissue specimens (patients information in Table 2), we performed the immunofluorescence staining and the results shown that CD80 was significantly downregulated in recurrence GBM tissues than the primary GBM tissues, while CD206 was *in verse* (Fig. 1B). Due to the limitations of the tissue samples, we evaluated the correlation of CD80 expression level and patients' survival based on the information in TCGA database. The heat map revealed a linear reverse relationship between CD80 and tumor proliferation and metastasis indicators (BIRC5,MYC, and MMP9, Fig. 1C), which suggested the negatively relationship between with GBM progression and M1-like polarization of microglia.

Interestingly, we noticed a similar trend of expression level between CD80 and EphA2 in the TCGA database (Fig. 1C). Using the GBM patient tissue specimens, we found the expression level of EphA2 was

also higher in the primary GBM tissues than the recurrence GBM tissues, indicating the potential correlation between EphA2 and M1-like polarization of microglia (Fig. 1D).

GBM cells prevented EphA2 expression and M1-like polarization of microglia

The polarization of microglia and protein expression is regulated by both instinct and external factors. We next assessed the role of GBM cells in determining EphA2 expression and polarization of microglia using the co-culture system (Fig. 2A). Co-cultured BV2 with the GBM cells (GL261 or C6) for the indicated time, qPCR shown that the expression level of CD80 in BV2 was downregulated in a time dependent manner in the presence of GL261 or C6, while the Arg-1 and CD206 were upregulated (Fig. 2B), which suggested GBM cells prevented M1-like polarization of microglia.

Moreover, co-cultured BV2 with GL261 or C6, the expression level of EphA2 in BV2 was significantly down-regulated in a time dependent manner with the peak inhibition at 24 h (Fig. 2C and 2D). The similar results can also be acquired by immunofluorescence staining (Fig. 2E), indicating GBM cells inhibited EphA2 in microglia.

Epha2 Promoted The M1-like Polarization Of Bv2

To investigate the role of EphA2 in microglia polarization, we first transfected EphA2 cDNA plasmid into BV2 cells and confirmed the overexpression of EphA2 proteins in these cells by western blot and qPCR (Fig. 3A and 3B). qPCR shown that iNOS significantly upregulated, while CD206 and Arg-1 downregulated in EphA2 overexpression BV2 cell (Fig. 3C). The similar results can also be acquired in the sorted primary microglia (Fig. 3D). Western blot shown the expression level of iNOS, TNF-α and IL-1β in EphA2 overexpression BV2 cell increased (Fig. 3E). These results indicated that EphA2 induce M1-like polarization of microglia.

To further elucidate the functional role EphA2 in BV2 polarization, two stable EphA2-knockdown cell clones (EphA2 shRNA1 and shRNA2) were established, and high silencing efficiency (90% silencing) was confirmed by western blot (Figure S1). Compared to the parental cancer cells, EphA2 knockdown cells showed the upregulation of CD206 and Arg-1, and downregulation of iNOS at the RNA level (Fig. 3F). Western blot shown the expression level of iNOS, TNF-α and IL-1β in EphA2 knockdown BV2 cell decreased (Fig. 3G). These results demonstrated knockdown EphA2 prevented M1-like polarization of microglia. Moreover, NLRP3 expression level increased in EphA2 overexpression BV2 cells, and decreased in EphA2-knockdown BV2 cells, which indicated that EphA2 was also involved in the inflammation response (Fig. 3E and G).

To further confirmed the role of EphA2 induced M1-like polarization of microglia in GBM cells metastasis, we performed Transwell migration and invasion assays. Co-cultured with EphA2 overexpression BV2 cells, the number of living C6 and GL261 GBM cells that passed through the membrane was much lower than the number of the cells for the control group (Fig. 3H-K). These results supported the hypothesis that

EphA2 induced M1-like polarization of microglia prevents the invasion and metastasis potential of living GBM cells.

PI3K/Akt pathway is involved in EphA2-mediated M1-like polarization of BV2

To further understand the underlying mechanism of EphA2 regulating microglia polarization, iTRAQ labeling was firstly used to identify differentially expressed phosphorylated proteins. iTRAQ-LC-MS/MS analysis results demonstrated that a total of 2,232 phosphorylated proteins, 4,941 phosphorylated peptides and 7,136 phosphorylated sites were identified (Fig. 4A). A total of 443 quantified proteins with $P < 0.05$ and an expression change greater than 2-fold or less than 0.5-fold between the KO and control groups were manually selected. Compared with the control group, 370 proteins were upregulated and 73 were downregulated (Fig. 4B). To better understand the involvement of EphA2 in physiological functions in BV2 cells, Blast2 go software was used to determine all different phosphorylated peptides, and a GO functional enrichment analysis of proteins corresponding to the phosphorylated peptides was then performed by Fisher. The results demonstrated that EphA2 involved nucleic acid binding, intracellular organelles, nucleoplasm and organelles (data not shown). KEGG pathway enrichment analysis revealed that 21 phosphorylated peptides were related to PI3K-AKT pathway (Fig. 4C and 4D).

As the PI3K-AKT is an important regulator of macrophage polarization, we hypothesized that it may function downstream of EphA2 to mediate the M1-like polarization of BV2. To test this hypothesis, we assessed the PI3K-AKT pathway related proteins in the EphA2-knockdown, EphA2-overexpression and parental BV2 cells. Compared to the parental BV2 cells, the expression level of p-PI3K and p-AKT was significantly increased in EphA2-overexpression BV2 cells (Fig. 4E-F), while the significantly decreased expression of p-PI3K and p-AKT in EphA2-knockdown BV2 cells was observed (Fig. 4G-H).

To further confirm the role of PI3K-AKT pathway in EphA2 mediated the M1-like polarization of BV2, PI3K-AKT pathway activator, sc-79, was also used. As expected, the expression level of p-PI3K and p-AKT was increased in BV2 cells in the presence of sc-79 (Fig. S2). Treated EphA2-knockdown BV2 cells with sc-79, the expression level of CD80 and IL-6 was significantly upregulated, while Arg-1 was downregulated as assessed by RT-PCR (Fig. 4I). Moreover, co-cultured with EphA2-knockdown BV2 cells in the presence of sc-79, the ability of C6 and GL261 metastasis and invasion was significantly inhibited (Fig. 4J).

EphA2-mediated M1-like polarization of BV2 inhibited GBM cells proliferation and metastasis in vivo

To validate our *in vitro* observation EphA2-mediated M1-like polarization of microglia inhibiting GBM cells metastasis, we performed tumor growth and metastasis assays *in vivo.* We firstly tested examined the metastasis of GMB cells in nude mice by injecting 1×10^6 C6 cells co-cultured with BV2 cells (control group) or EphA2 overexpression BV2 cells into the mouse tail vein. From the HE staining, we observed that C6 cells exposed to EphA2 overexpression BV2 cells showed significantly more and larger metastatic foci than the control group (Fig. 5A). Moreover, we also assessed the proliferation ability of GMB cells in nude mice by injecting 1×10^6 C6 cells co-cultured with BV cells (control group) or EphA2 overexpression BV2 cells. As shown in Fig. 5B-D, tumors from EphA2 overexpression BV2 cells co-culture group grew

slower and smaller than the control group, and larger necrotic area was also observed from the HE staining. Moreover, there was a significant reduction of proliferation (survivin and c-myc) and metastasis (ZEB1 and β-catenin) related markers in protein expression level (Fig. 5E). These *in vivo* results further supported the *in vitro* evidence that EphA2-mediated M1-like polarization of microglia prevented GBM cells metastasis.

Discussion

In the present study, we demonstrated that EphA2 expressed on microglia from the GMB patients and orthotopic tumor tissue. Elevated EphA2 promoted the M1-like polarization and prevented M2-like polarization of microglia. EphA2 activates PI3K/ AKT in microglia, which is important signaling events underlying M1-like polarization of microglia. Furthermore, EphA2 induced the M1-like polarization of microglia attenuated the migration and invasion of GBM cells *in vitro* and *in vivo* (Fig. 6); therefore, activating EphA2 may contribute to the GBM inhibition tumor microenvironment.

As the main innate immune cells of the CNS, the primary goal of microglia is to maintain homeostasis[20]. In the GBM microenvironment, microglia and macrophages have been designated as M1- or M2-polarized cells in response to pro-inflammatory and anti-inflammatory cytokines[21, 22]. Although this definition was over-simplified, they are actually histologically indistinguishable from each other and still widely used in the research. In this study, we used the common accepted marker to definition M1 polarized cells according to the previously publication[23, 24]. It was confirmed that M2-like polarization of microglia contributed to thetumor progression and reduces survival, while M1-like polarization of microglia *in verse*. The polarization of microglia is determined by the external and instinct factors, but the exact underlying mechanisms are still unclear. In our study, M1-like polarization of microglia was influenced by the surrounding and the expression level of EphA2. However, the exact avenue of GBM cells regulated the polarization of microglia still need further deeper investigation and exosome may play a critical role in the process. In the ischemic stroke model, LPS-exo exhibited potent anti-inflammatory and neuroprotective roles by skewing microglia polarity from the M1 phenotype to the M2 phenotype[25]. In multiple sclerosis (MS), BMSC-derived exosomes attenuated inflammation and demyelination of the CNS by regulating microglia polarization in an EAE animal model[26].

Under normal condition, EphA2 expression is mainly restricted to proliferating epithelial cells[27]. While EphA2 is upregulated at the gene and protein levels in human tumor tissue specimens, especially the highest malignancy tumors[28]. Therefore, overexpression and aggressive features of EphA2 in tumor cells and relatively low expression in most normal adult tissues make this protein a potential therapeutic target in cancer. Several EphA2 target therapy strategies had been developed in cancer treatment, such as blocking its expression and activation, promoting its degradation, or EphA2-based immunotherapy[29–31]. Suppression EphA2 in GBM cells displayed multiple malignant features inhibition, including impaired anchorage independent growth, proliferation, and migration[32].Yamaguchi et al. developed a Dendritic cell (DC)-based vaccine pulsed with EphA2-derived peptide (Eph-DCs) which shown a promise colorectal cancer inhibition effect[33].In our study, EphA2 expressed on microglia induced M1-like polarization of

this subpopulation. Moreover, EphA2-metdiated the M1-like of microglia inhibited the GBM metastasis and growth. Therefore, the exact role of EphA2 in tumor is context dependent and its target therapy still need further evaluation before clinical translation.

In summary, we identified EphA2-PI3K-Akt signaling pathway as a driver for M1-like polarization of microglia, which further attenuated the migration and metastasis of GMB cells in vitro and in vivo. As the widely accepted concept of target EphA2 in cancer therapeutic intervention, our research provided a new information to rationale for targeting EphA2 to improve treatment outcomes in glioblastoma cancer.

Conclusion

M2 microglial polarization was associated with decreased EphA2 expression in microglia cocultured with GBM cells. BV2 cells displayed an M1 phenotype when EphA2 was overexpressed and an M2 phenotype when EphA2 was knocked down via PI3K-AKT pathway. Furthermore, EphA2 overexpression in BV2 cells inhibited GBM cell migration and invasion. In conclusion, our study confirmed that EphA2 promoted M1 microglia polarization, which blocked to glioma progression. This study further explains the mechanism of microglia polarization and provides an effective therapeutic target for the clinical treatment of GBM.

Abbreviations

glioblastoma multiforme GBM

central nervous system CNS

polyvinylidenedifluoride PVDF

electrochemiluminescence ECL

peritumoral edema PTBE

receptor tyrosine kinases RTK

Eph receptor A2 EphA2

isobaric tags for relative and absolute quantification iTRAQ

quantitative real-time PCR qPCR

Dulbecco's modified Eagle's medium DMEM

fetal bovine serum FBS

tumor-associated macrophages TAMs

Declarations

Ethics approval and consent to participate

The animal experiments conducted strictly in line with the Animal StudyGuidelines of Nanjing University.

Consent for publication

All authors have agreed to the publication of the article.

Availability of data and materials

The data supporting the findings of this study are included in this paper andits additional files

Competing interests

The authors have declared that no conflict of interest exists.

Funding

This study was supported by the National Natural Science Foundation of China (grant numbers 81530054 and 81971681) and National Natural Science Foundation of China Youth Fund (grant number 81701770).

Authors' contributions

XL and YT carried out the molecular studies. XL and RF carried out the transwell assay. CC and ZJW provided patients tissues. XXL, JS, and ML carried out test operation in animal experiment and cell experiment. JRL carried out measurements. XL wrote the manuscript. GML, YT and RF revised the manuscript. JRL and GML gave scientific advices. All the authors contributed through scientific discussion and reviewed the manuscript. The author(s) read and approved the final manuscript.

Acknowledgements

We would like to acknowledge our lab colleagues for their support in thedevelopment of this article.

References

1. Okada M, Saio M, Kito Y, Ohe N, Yano H, Yoshimura S, Iwama T, Takami T. Tumor-associated macrophage/microglia infiltration in human gliomas is correlated with MCP-3, but not MCP-1. Int J Oncol. 2009;34:1621–7.
2. Charles NA, Holland EC, Gilbertson R, Glass R, Kettenmann H. The brain tumor microenvironment. Glia. 2012;60:502–14.

3. Poon CC, Sarkar S, Yong VW, Kelly JJP. Glioblastoma-associated microglia and macrophages: targets for therapies to improve prognosis. Brain. 2017;140:1548–60.
4. Martinez FO, Sica A, Mantovani A, Locati M. Macrophage activation and polarization. Front Biosci. 2008;13:453–61.
5. Hambardzumyan D, Gutmann DH, Kettenmann H. The role of microglia and macrophages in glioma maintenance and progression. Nat Neurosci. 2016;19:20–7.
6. Wei J, Gabrusiewicz K, Heimberger A. The controversial role of microglia in malignant gliomas. Clin Dev Immunol 2013; 2013: 285246.
7. Ireton RC, Chen J. EphA2 receptor tyrosine kinase as a promising target for cancer therapeutics. Curr Cancer Drug Targets. 2005;5:149–57.
8. Pasquale EB. Eph-ephrin bidirectional signaling in physiology and disease. Cell. 2008;133:38–52.
9. Miao H, Wang B. EphA receptor signaling–complexity and emerging themes. Semin Cell Dev Biol. 2012;23:16–25.
10. Kinch MS, Moore MB, Harpole DH. Jr. Predictive value of the EphA2 receptor tyrosine kinase in lung cancer recurrence and survival. Clin Cancer Res. 2003;9:613–8.
11. Garcia-Monclús S, López-Alemany R, Almacellas-Rabaiget O, Herrero-Martín D, Huertas-Martinez J, Lagares-Tena L, Alba-Pavón P, Hontecillas-Prieto L, Mora J, de Álava E, Rello-Varona S, Giangrande PH, Tirado OM. EphA2 receptor is a key player in the metastatic onset of Ewing sarcoma. Int J Cancer. 2018;143:1188–201.
12. Zelinski DP, Zantek ND, Stewart JC, Irizarry AR, Kinch MS. EphA2 overexpression causes tumorigenesis of mammary epithelial cells. Cancer Res. 2001;61:2301–6.
13. Li Z, Tanaka M, Kataoka H, Nakamura R, Sanjar R, Shinmura K, Sugimura H. EphA2 up-regulation induced by deoxycholic acid in human colon carcinoma cells, an involvement of extracellular signal-regulated kinase and p53-independence. J Cancer Res Clin Oncol. 2003;129:703–8.
14. Hamaoka Y, Negishi M, Katoh H. EphA2 is a key effector of the MEK/ERK/RSK pathway regulating glioblastoma cell proliferation. Cell Signal. 2016;28:937–45.
15. Xiao T, Xiao Y, Wang W, Tang YY, Xiao Z, Su M. Targeting EphA2 in cancer. J Hematol Oncol. 2020;13:114.
16. Frei K, Bodmer S, Schwerdel C, Fontana A. Astrocyte-derived interleukin 3 as a growth factor for microglia cells and peritoneal macrophages. J Immunol. 1986;137:3521–7.
17. Wisniewski JR, Zougman A, Nagaraj N, Mann M. Universal sample preparation method for proteome analysis. Nat Methods. 2009;6:359–62.
18. Larsen MR, Thingholm TE, Jensen ON, Roepstorff P, Jorgensen TJ. Highly selective enrichment of phosphorylated peptides from peptide mixtures using titanium dioxide microcolumns. Mol Cell Proteomics. 2005;4:873–86.
19. Taus T, Köcher T, Pichler P, Paschke C, Schmidt A, Henrich C, Mechtler K. Universal and confident phosphorylation site localization using phosphoRS. J Proteome Res. 2011;10:5354–62.

20. Ostrom QT, Bauchet L, Davis FG, Deltour I, Fisher JL, Langer CE, Pekmezci M, Schwartzbaum JA, Turner MC, Walsh KM, Wrensch MR, Barnholtz-Sloan JS. The epidemiology of glioma in adults: a "state of the science" review. Neuro Oncol. 2014;16:896–913.
21. Mills CD, Kincaid K, Alt JM, Heilman MJ, Hill AM. M-1/M-2 macrophages and the Th1/Th2 paradigm. J Immunol. 2000;164:6166–73.
22. Gordon S. Alternative activation of macrophages. Nat Rev Immunol. 2003;3:23–35.
23. Prosniak M, Harshyne LA, Andrews DW, Kenyon LC, Bedelbaeva K, Apanasovich TV, Heber-Katz E, Curtis MT, Cotzia P, Hooper DC. Glioma grade is associated with the accumulation and activity of cells bearing M2 monocyte markers. Clin Cancer Res. 2013;19:3776–86.
24. Ueda R, Fujita M, Zhu X, Sasaki K, Kastenhuber ER, Kohanbash G, McDonald HA, Harper J, Lonning S, Okada H. Systemic inhibition of transforming growth factor-beta in glioma-bearing mice improves the therapeutic efficacy of glioma-associated antigen peptide vaccines. Clin Cancer Res. 2009;15:6551–9.
25. Horvath RJ, Nutile-McMenemy N, Alkaitis MS, Deleo JA. Differential migration, LPS-induced cytokine, chemokine, and NO expression in immortalized BV-2 and HAPI cell lines and primary microglial cultures. J Neurochem. 2008;107:557–69.
26. Li Z, Liu F, He X, Yang X, Shan F, Feng J. Exosomes derived from mesenchymal stem cells attenuate inflammation and demyelination of the central nervous system in EAE rats by regulating the polarization of microglia. Int Immunopharmacol. 2019;67:268–80.
27. Héroult M, Schaffner F, Augustin HG. Eph receptor and ephrin ligand-mediated interactions during angiogenesis and tumor progression. Exp Cell Res. 2006;312:642–50.
28. Ieguchi K, Maru Y. Roles of EphA1/A2 and ephrin-A1 in cancer. Cancer Sci. 2019;110:841–8.
29. Hannon GJ, Rossi JJ. Unlocking the potential of the human genome with RNA interference. Nature. 2004;431:371–8.
30. Zhou Z, Yuan X, Li Z, Tu H, Li D, Qing J, Wang H, Zhang L. RNA interference targeting EphA2 inhibits proliferation, induces apoptosis, and cooperates with cytotoxic drugs in human glioma cells. Surg Neurol. 2008;70:562–8. discussion 568–569.
31. Pecot CV, Calin GA, Coleman RL, Lopez-Berestein G, Sood AK. RNA interference in the clinic: challenges and future directions. Nat Rev Cancer. 2011;11:59–67.
32. Wykosky J, Palma E, Gibo DM, Ringler S, Turner CP, Debinski W. Soluble monomeric EphrinA1 is released from tumor cells and is a functional ligand for the EphA2 receptor. Oncogene. 2008;27:7260–73.
33. Yamaguchi S, Tatsumi T, Takehara T, Sakamori R, Uemura A, Mizushima T, Ohkawa K, Storkus WJ, Hayashi N. Immunotherapy of murine colon cancer using receptor tyrosine kinase EphA2-derived peptide-pulsed dendritic cell vaccines. Cancer. 2007;110:1469–77.

Tables

Due to technical limitations, table 1 and 2 is only available as a download in the Supplemental Files section.

Figures

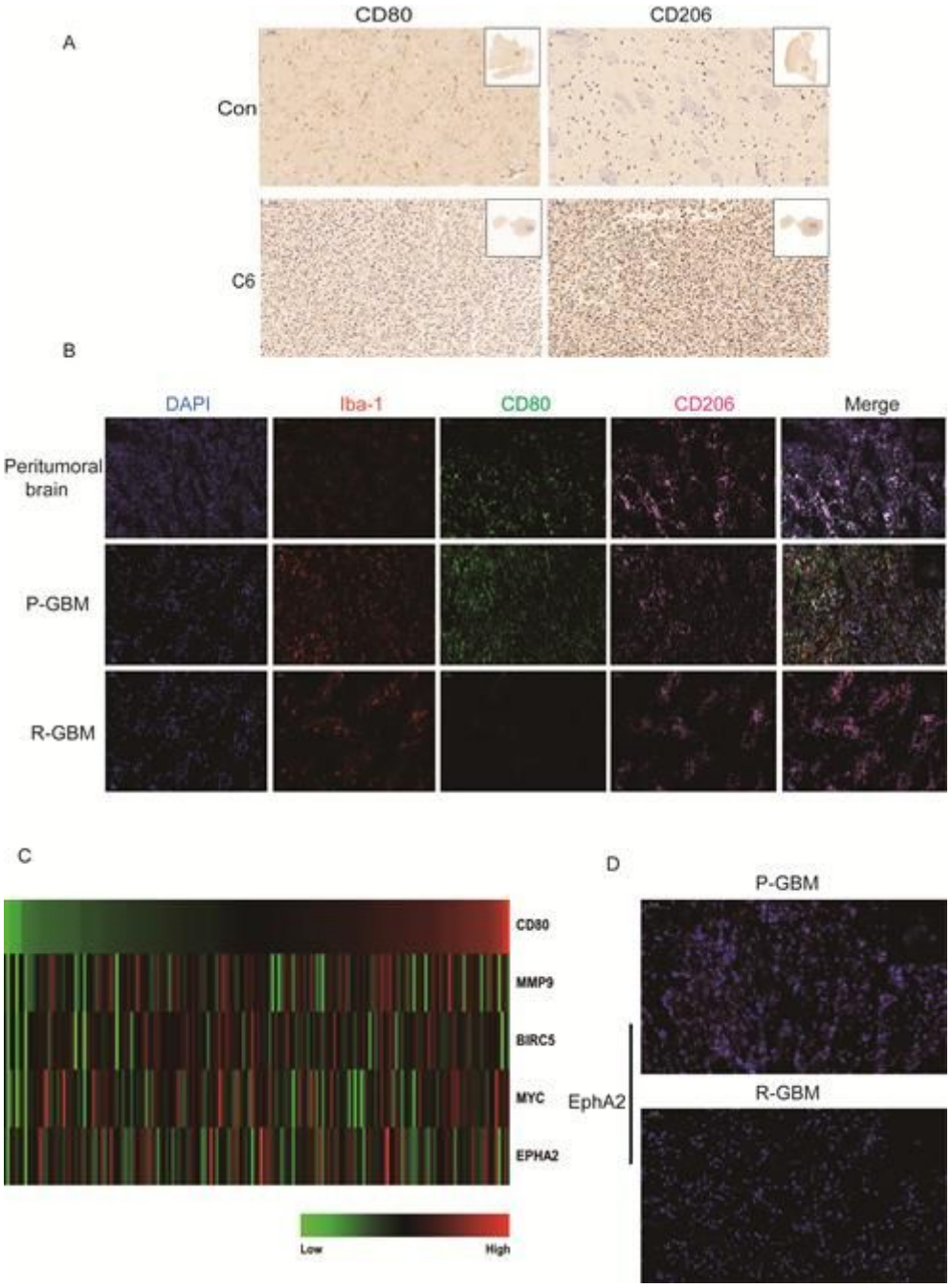

Figure 1

M1-like polarization of microglia negatively correlation with GBM progression. (A) Immunohistochemical staining assessed the expression of CD80 and CD206 on the mice normal and GBM orthotopic tumor tissue. Magnification: × 4 and × 10.(B) Immunofluorescence staining analysis the co-localization of Iba-1(red), CD80(green) and CD206(pink) on primary and recurrence of GBM patient grossspecimen. scale

bar50μm. (C) Analysis of the relationships between CD80 and MMP9, BIRC5, MYC and EphA2 expression in human GBM cancer tissues from the TCGA database. The results were presented by heat map (n=172). (D) Immunofluorescence staining assessed the expression level of EphA2 on primary and recurrence of GBM patient gross specimen. scale bar 50 μm. Experiments were repeated three times, and the data were expressed as the mean ± SEM. * p< 0.05, ** p< 0.01, *** p< 0.001 vs. control group. Statistical analysis was performed using Student's t-test and Pearson correlation analysis.

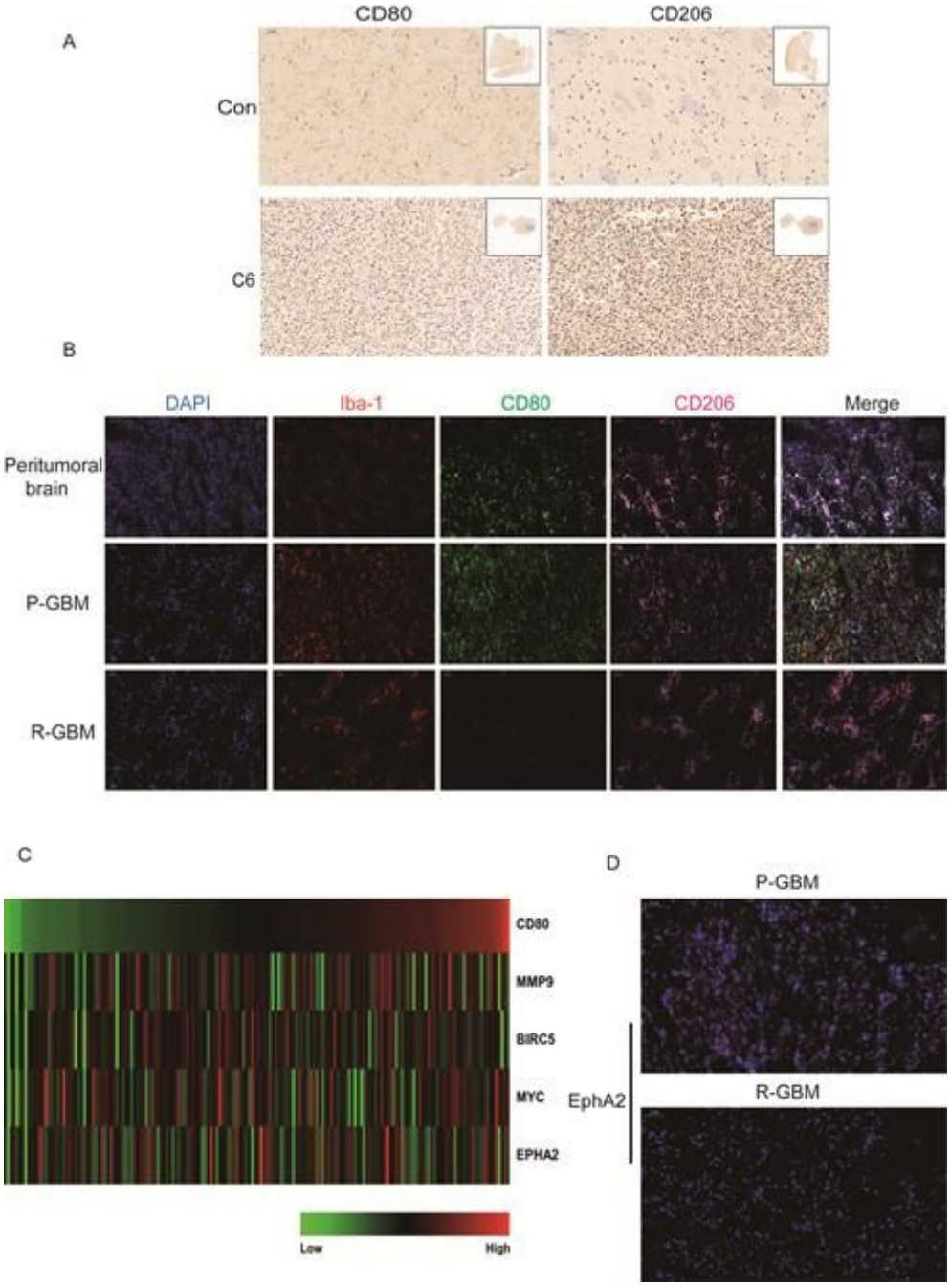

Figure 1

M1-like polarization of microglia negatively correlation with GBM progression. (A) Immunohistochemical staining assessed the expression of CD80 and CD206 on the mice normal and GBM orthotopic tumor tissue. Magnification: × 4 and × 10.(B) Immunofluorescence staining analysis the co-localization of Iba-

1(red), CD80(green) and CD206(pink) on primary and recurrence of GBM patient grossspecimen. scale bar50μm. (C) Analysis of the relationships between CD80 and MMP9, BIRC5, MYC and EphA2 expression in human GBM cancer tissues from the TCGA database. The results were presented by heat map (n=172). (D) Immunofluorescence staining assessed the expression level of EphA2 on primary and recurrence of GBM patient gross specimen. scale bar 50 μm. Experiments were repeated three times, and the data were expressed as the mean ± SEM. * p< 0.05, ** p< 0.01, *** p< 0.001 vs. control group. Statistical analysis was performed using Student's t-test and Pearson correlation analysis.

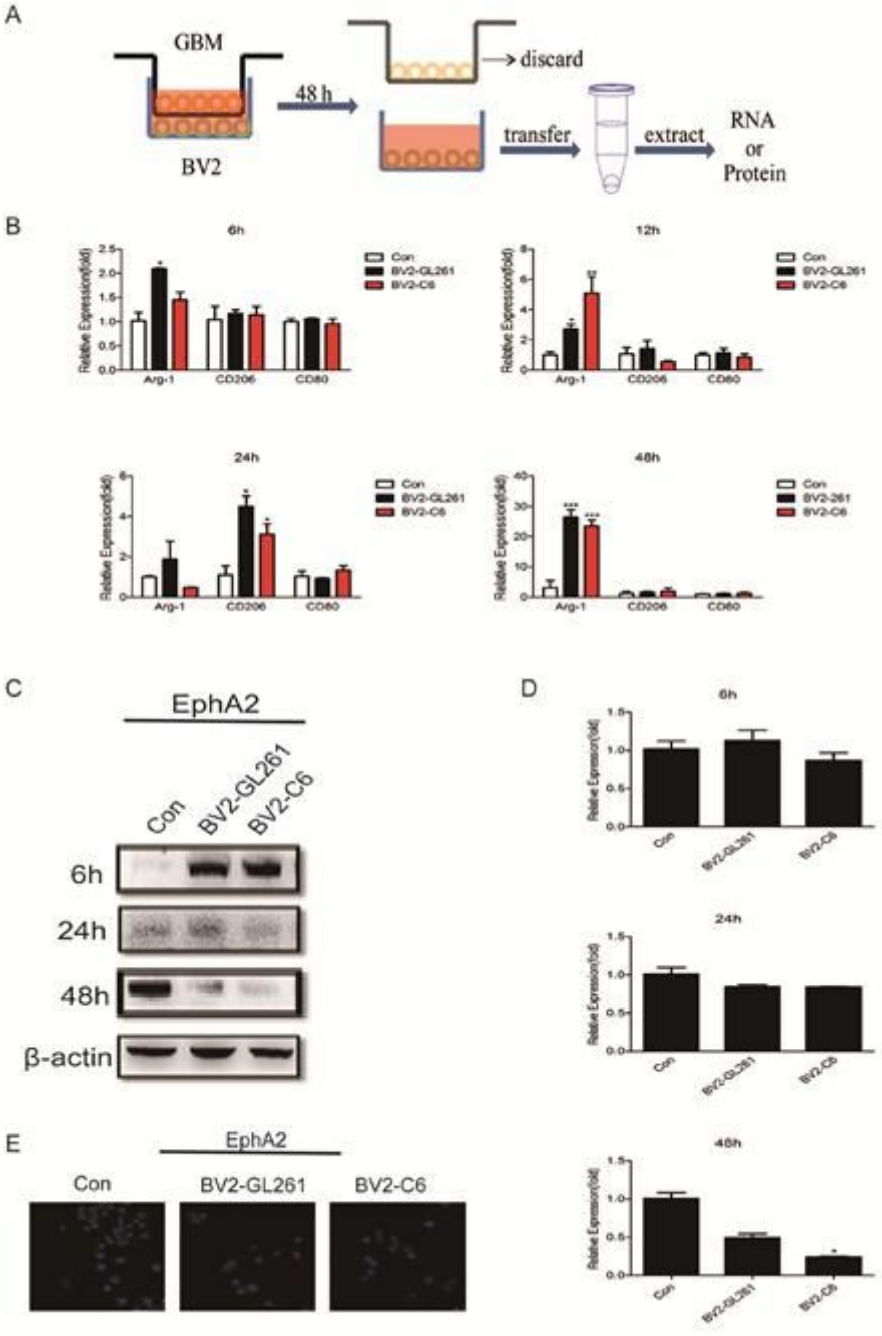

Figure 2

GBM cells prevented EphA2 expression and M1-like polarization of microglia. (A) Schematic representation of the in vitro co-culture system of GBM cells and BV2 cells. (B, C) Western blot and

quantitative analysis of the protein expression levels of EphA2 on BV cells following co-cultured with GL261 or C6 for the indicated time (0, 6, 24 and 48 h). β-actin was detected as a loading control.(D) Immunofluorescence staining assessed the expression level of EphA2 on BV cells following co-cultured with or without GL261 or C6 for 24h. Experiments were repeated three times, and the data were expressed as the mean ± SEM. * p< 0.05, ** p< 0.01, *** p< 0.001 vs. control group. Statistical analysis was performed using Student's t-test.

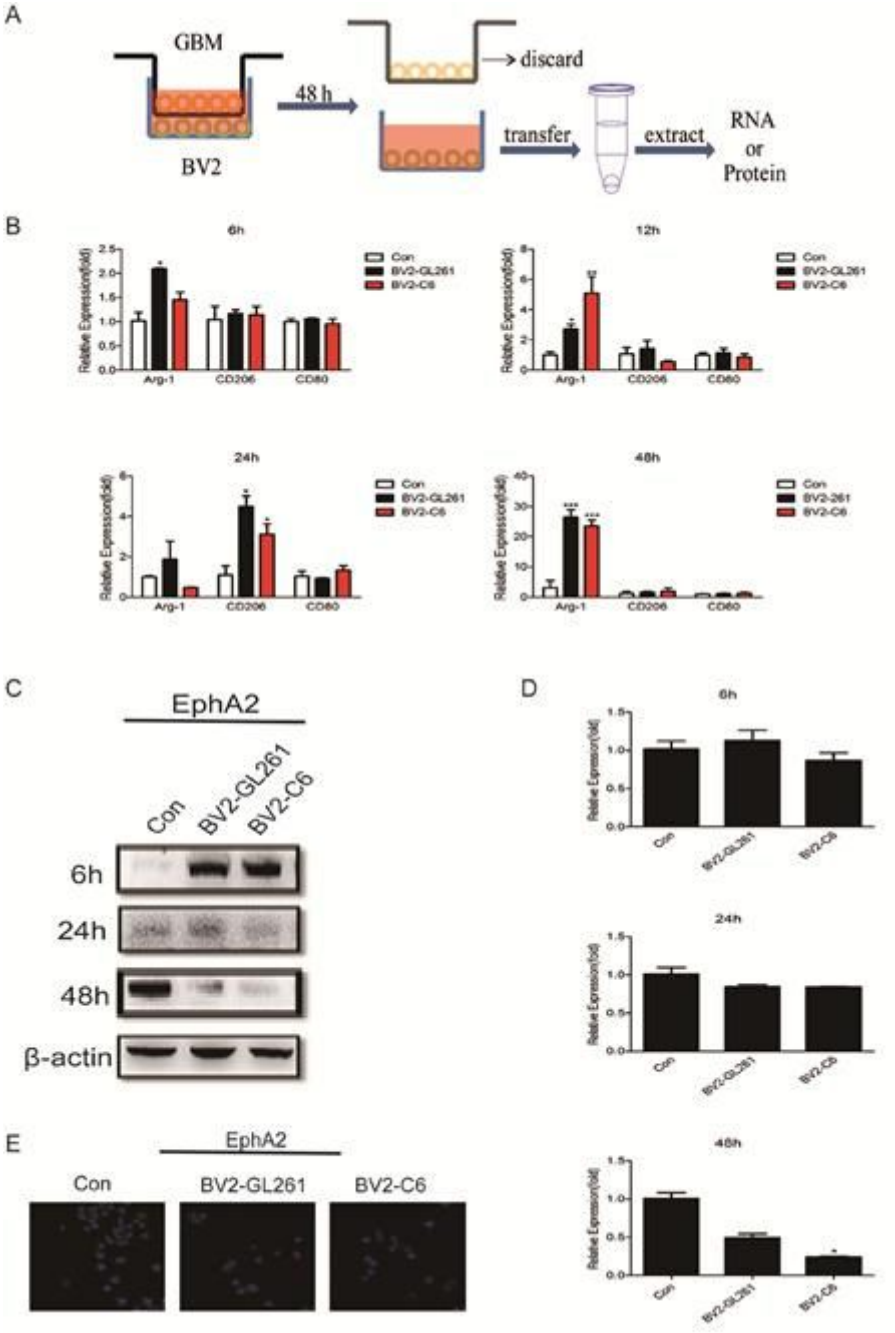

Figure 2

GBM cells prevented EphA2 expression and M1-like polarization of microglia. (A) Schematic representation of the in vitro co-culture system of GBM cells and BV2 cells. (B, C) Western blot and quantitative analysis of the protein expression levels of EphA2 on BV cells following co-cultured with

GL261 or C6 for the indicated time (0, 6, 24 and 48 h). β-actin was detected as a loading control.(D) Immunofluorescence staining assessed the expression level of EphA2 on BV cells following co-cultured with or without GL261 or C6 for 24h. Experiments were repeated three times, and the data were expressed as the mean ± SEM. * p< 0.05, ** p< 0.01, *** p< 0.001 vs. control group. Statistical analysis was performed using Student's t-test.

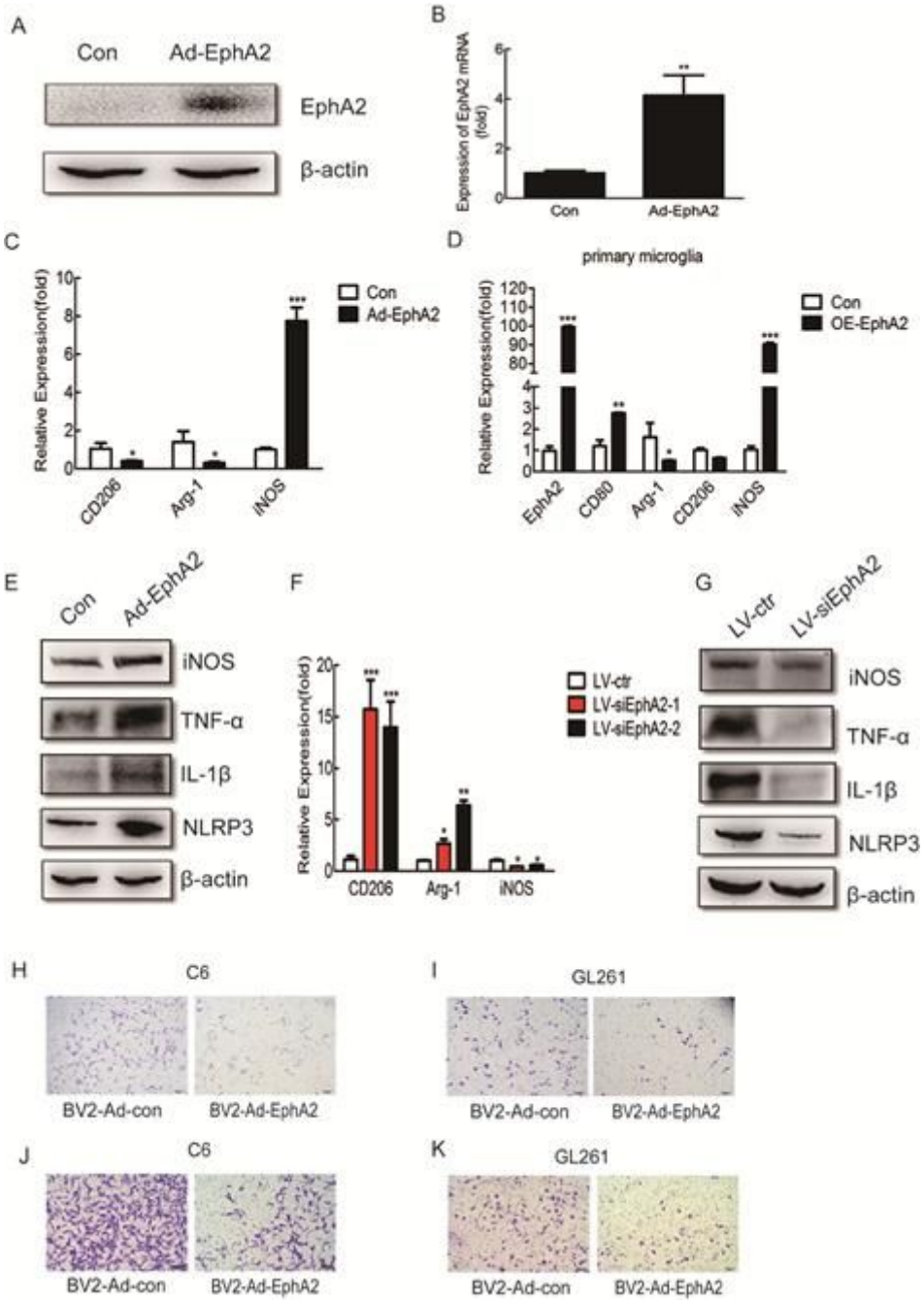

Figure 3

EphA2 promoted the M1-like polarization of BV2. (A, B) Western blot and quantitative analysis of EphA2 expression inEphA2overexpressed BV2 cells. (C, D) RT-PCR analyzing the expression of CD206, Arg-1, and iNOS in EphA2 overexpressed BV2 cells (C) and primary microglia (D). β-actin was detected as a loading control. (E) Western blot analysis of the protein expression levels of iNOS, TNF-α and IL-1β in EphA2

overexpressed BV2 cells. β-actin was detected as a loading control.(F) RT-PCR analyzing the expression of CD206, Arg-1, and iNOS in EphA2knockdown BV2 cells. β-actin was detected as a loading control.(G) Western blot analysis of the protein expression levels of iNOS, TNF-α and IL-1β in EphA2 knockdown BV2 cells. β-actin was detected as a loading control.(H, I) The invasion ability of C6 (H) and GL261 (I) cells following co-cultured with parental or EphA2 overexpression BV2 cells were detected by transwell assay. Magnification: × 200. (J, K) The migration ability of C6 (J) and GL261 (K) cells following co-cultured with parental or EphA2 overexpression BV2 cells were detected by transwell assay. Magnification: × 200. Experiments were repeated three times, and the data are present as the mean ± SEM. * p< 0.05, ** p< 0.01, *** p< 0.001 vs. control group. Statistical analysis was performed using Student's t-test.

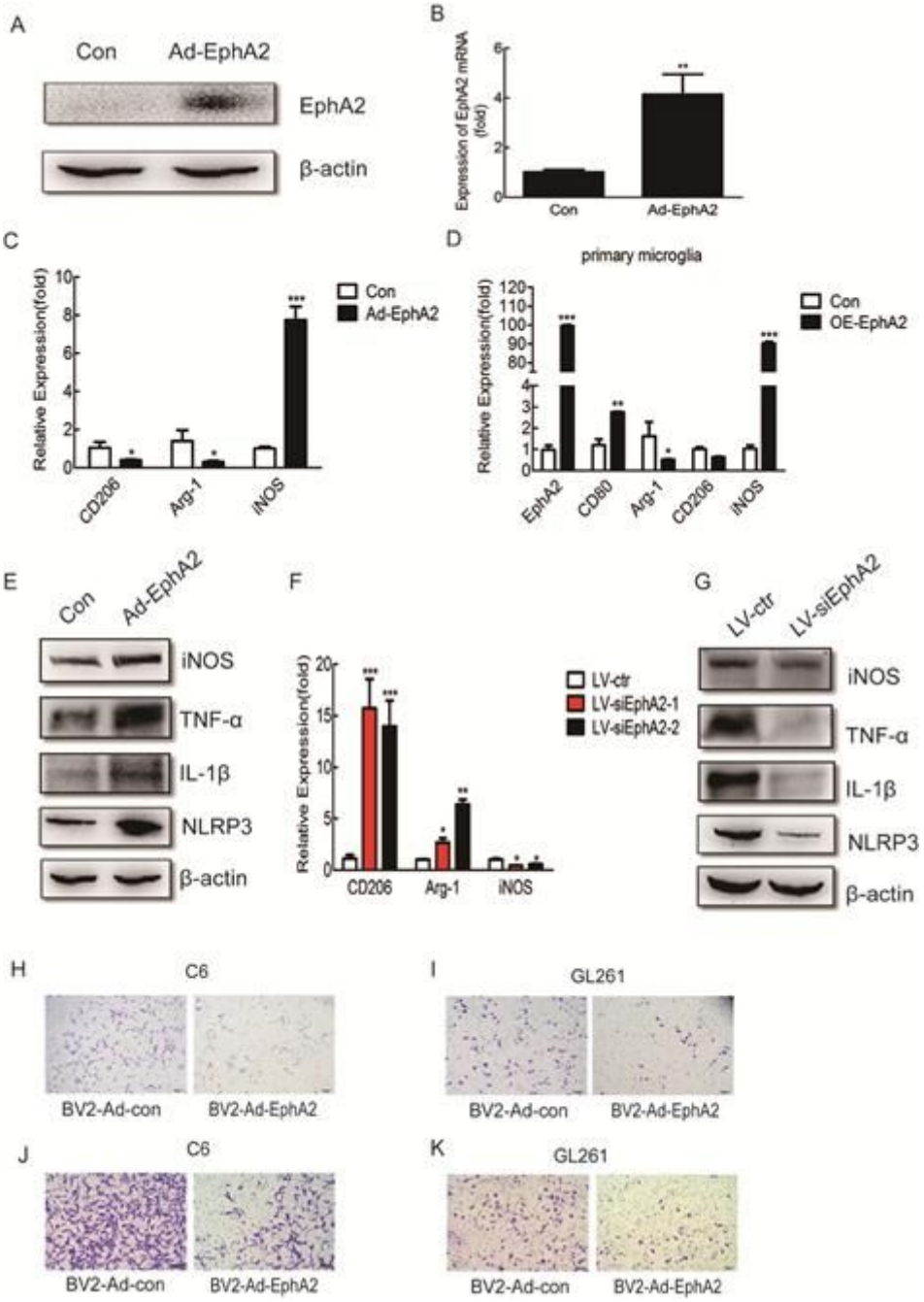

Figure 3

EphA2 promoted the M1-like polarization of BV2. (A, B) Western blot and quantitative analysis of EphA2 expression inEphA2overexpressed BV2 cells. (C, D) RT-PCR analyzing the expression of CD206, Arg-1, and iNOS in EphA2 overexpressed BV2 cells (C) and primary microglia (D). β-actin was detected as a loading control. (E) Western blot analysis of the protein expression levels of iNOS, TNF-α and IL-1β in EphA2 overexpressed BV2 cells. β-actin was detected as a loading control.(F) RT-PCR analyzing the expression of CD206, Arg-1, and iNOS in EphA2knockdown BV2 cells. β-actin was detected as a loading control.(G) Western blot analysis of the protein expression levels of iNOS, TNF-α and IL-1β in EphA2 knockdown BV2 cells. β-actin was detected as a loading control.(H, I) The invasion ability of C6 (H) and GL261 (I) cells following co-cultured with parental or EphA2 overexpression BV2 cells were detected by transwell assay. Magnification: × 200. (J, K) The migration ability of C6 (J) and GL261 (K) cells following co-cultured with parental or EphA2 overexpression BV2 cells were detected by transwell assay. Magnification: × 200. Experiments were repeated three times, and the data are present as the mean ± SEM. * $p< 0.05$, ** $p< 0.01$, *** $p< 0.001$ vs. control group. Statistical analysis was performed using Student's t-test.

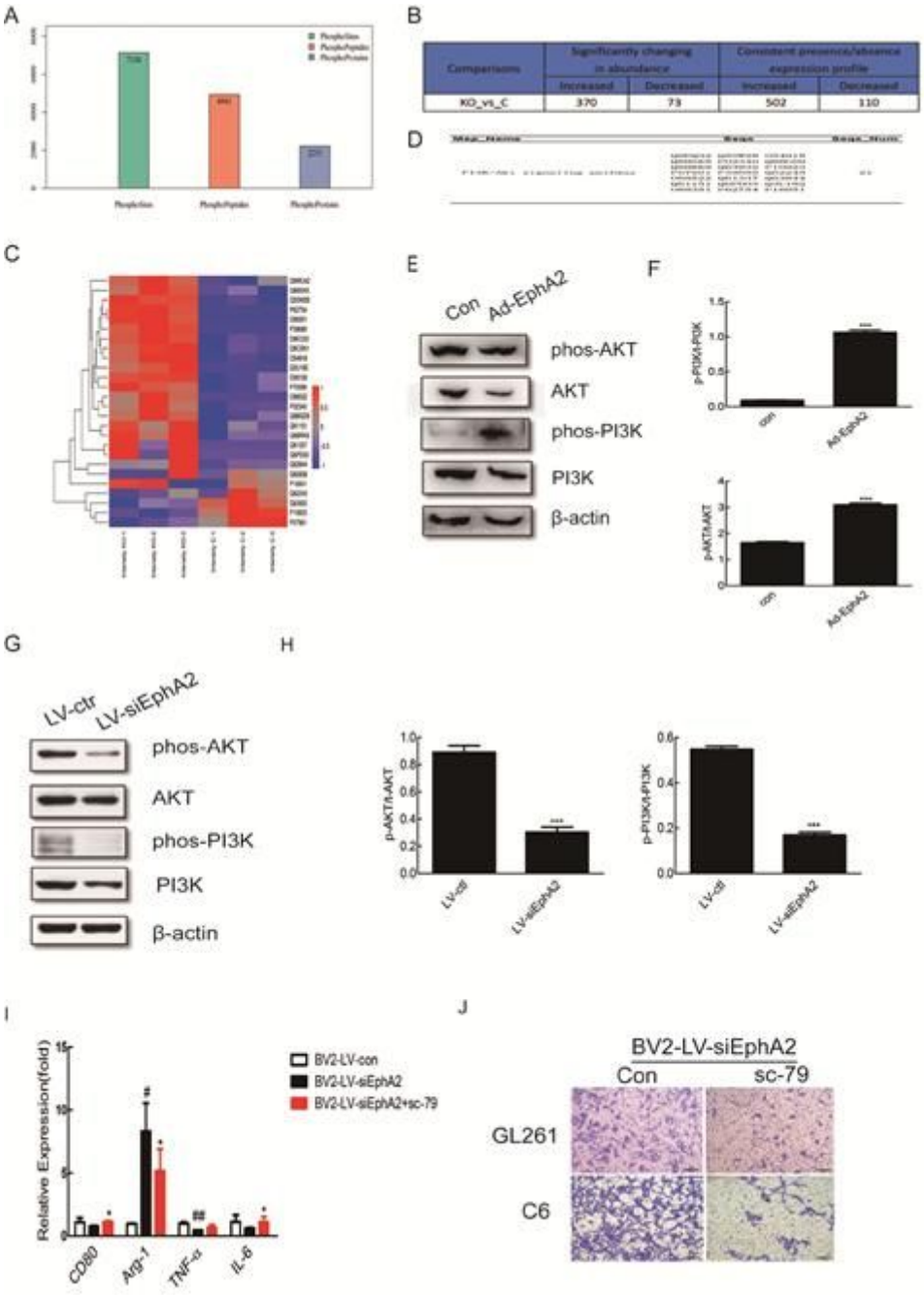

Figure 4

PI3K/Akt pathway is involved in EphA2-mediated M1-like polarization of BV2. (A, B) iTRAQ labeling and LC-MS/MS identified phosphorylated proteins,phosphorylated peptidesphosphorylated sites in EphA2 knockdown BV2 cells. (C) All phosphorylated proteins involved in the PI3K-AKT pathway. The results were presented by heat map. (D) Phosphorylated proteins involved in the PI3K-AKT pathway in EphA2 knockdown BV cells. (E, F) Western blot and quantitative analysis of the expression level of p-PI3K and p-Akt in parental or EphA2 overexpression BV2 cells. (G, H) Western blot and quantitative analysis of the expression of p-PI3K and p-Akt in parental orEphA2overexpression BV2 cells. β-actin was detected as a loading control. (I) RT-PCR analyzing the expression of CD80, Arg-1, TNF-α and IL-6 in parental or EphA2 knockdown BV2 cells in the presence or absence of sc-79 (PI3K activator). (J) The migration ability of C6

and GL261 cells following co-cultured with parental or EphA2 knockdown BV2 cells in the presence or absence of sc-79 were detected by transwell assay. Magnification: × 20. Experiments were repeated three times, and the data were expressed as the mean ± SEM. * p< 0.05, ** p< 0.01, *** p< 0.001 vs. control group. Statistical analysis was performed using Student's t-test.

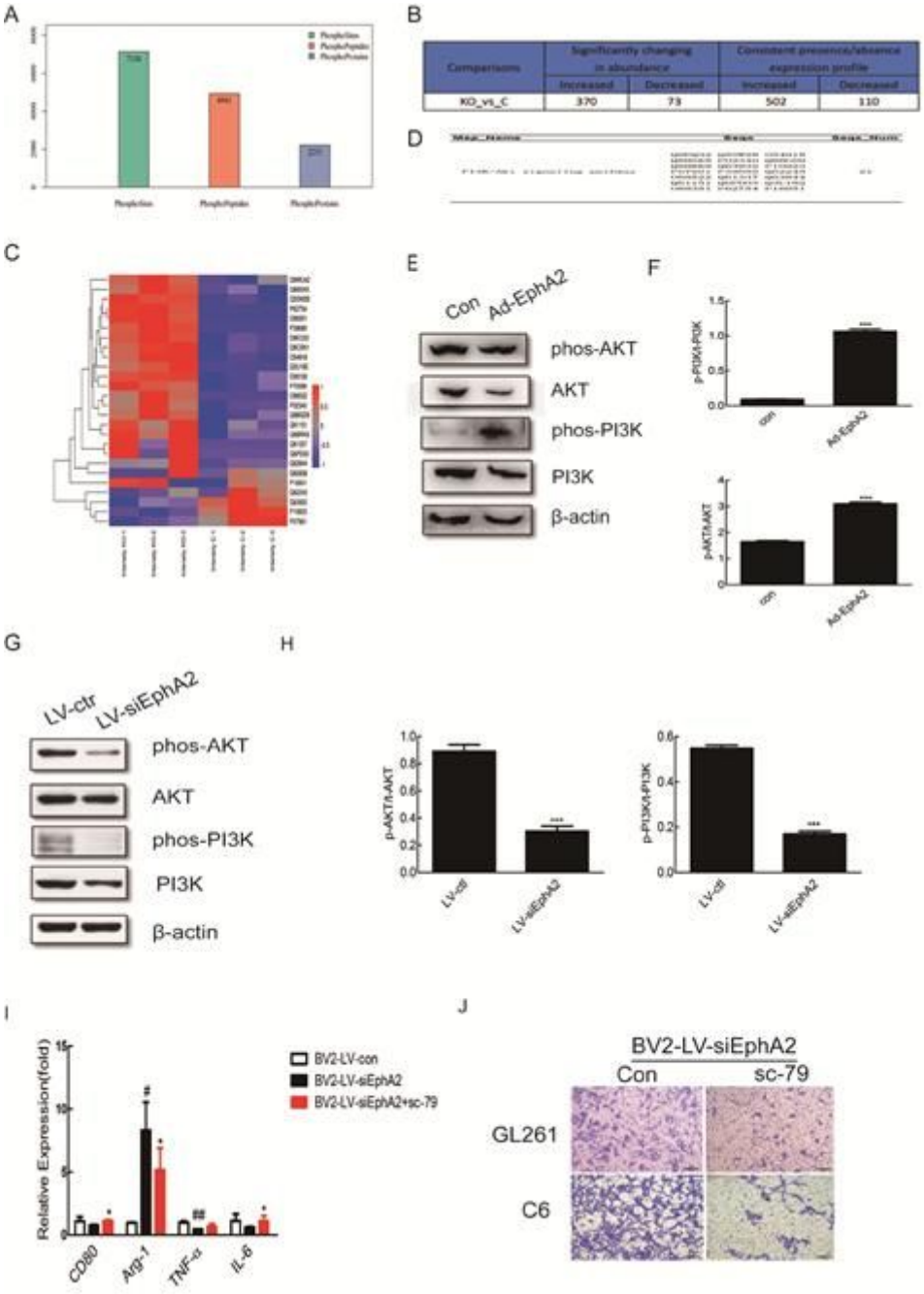

Figure 4

PI3K/Akt pathway is involved in EphA2-mediated M1-like polarization of BV2. (A, B) iTRAQ labeling and LC-MS/MS identified phosphorylated proteins,phosphorylated peptidesphosphorylated sites in EphA2 knockdown BV2 cells. (C) All phosphorylated proteins involved in the PI3K-AKT pathway. The results were presented by heat map. (D) Phosphorylated proteins involved in the PI3K-AKT pathway in EphA2 knockdown BV cells. (E, F) Western blot and quantitative analysis of the expression level of p-PI3K and p-

Akt in parental or EphA2 overexpression BV2 cells. (G, H) Western blot and quantitative analysis of the expression of p-PI3K and p-Akt in parental orEphA2overexpression BV2 cells. β-actin was detected as a loading control. (I) RT-PCR analyzing the expression of CD80, Arg-1, TNF-α and IL-6 in parental or EphA2 knockdown BV2 cells in the presence or absence of sc-79 (PI3K activator). (J) The migration ability of C6 and GL261 cells following co-cultured with parental or EphA2 knockdown BV2 cells in the presence or absence of sc-79 were detected by transwell assay. Magnification: × 20. Experiments were repeated three times, and the data were expressed as the mean ± SEM. * p< 0.05, ** p< 0.01, *** p< 0.001 vs. control group. Statistical analysis was performed using Student's t-test.

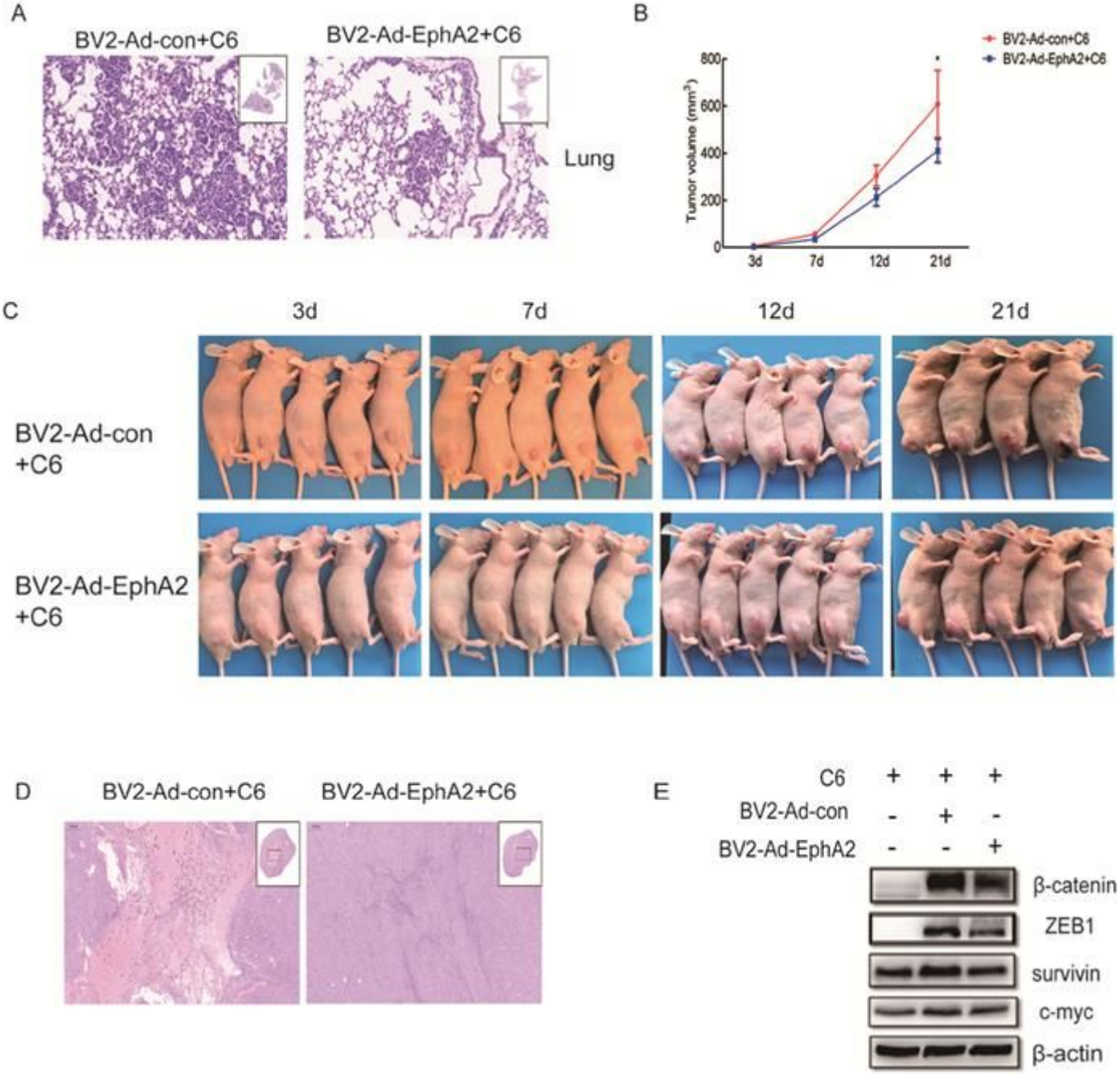

Figure 5

EphA2-mediated M1-like polarization of BV2 inhibited GBM cells proliferation and metastasis in vivo. (A) HE staining was used to verify the lung metastases foci of C6 co-cultured with parental or EphA2 overexpression BV2 cells. Magnification: × 4 and × 20. (B) Nude mice were injected subcutaneously with 1 × 106 C6 cells co-cultured with parental or EphA2 overexpression BV2 cells. Tumor volume was calculated for 3 weeks. (C) Representative photographs of tumor burden mice at the indicated time (3, 7, 12, 21d). (D) HE staining imaging of the necrosis area of subcutaneous tumor tissues at day 21 day after C6 injection. Magnification: × 20. (E) Western blot analysis of the protein expression level of ZEB1, β-catenin, survivin, and c-myc in the isolated tumor tissues. β-actin was detected as a loading control. Experiments were repeated three times, and the data are expressed as the mean ± SEM. * p< 0.05, ** p< 0.01, *** p< 0.001 vs. control group. Statistical analysis was performed using Student's t-test.

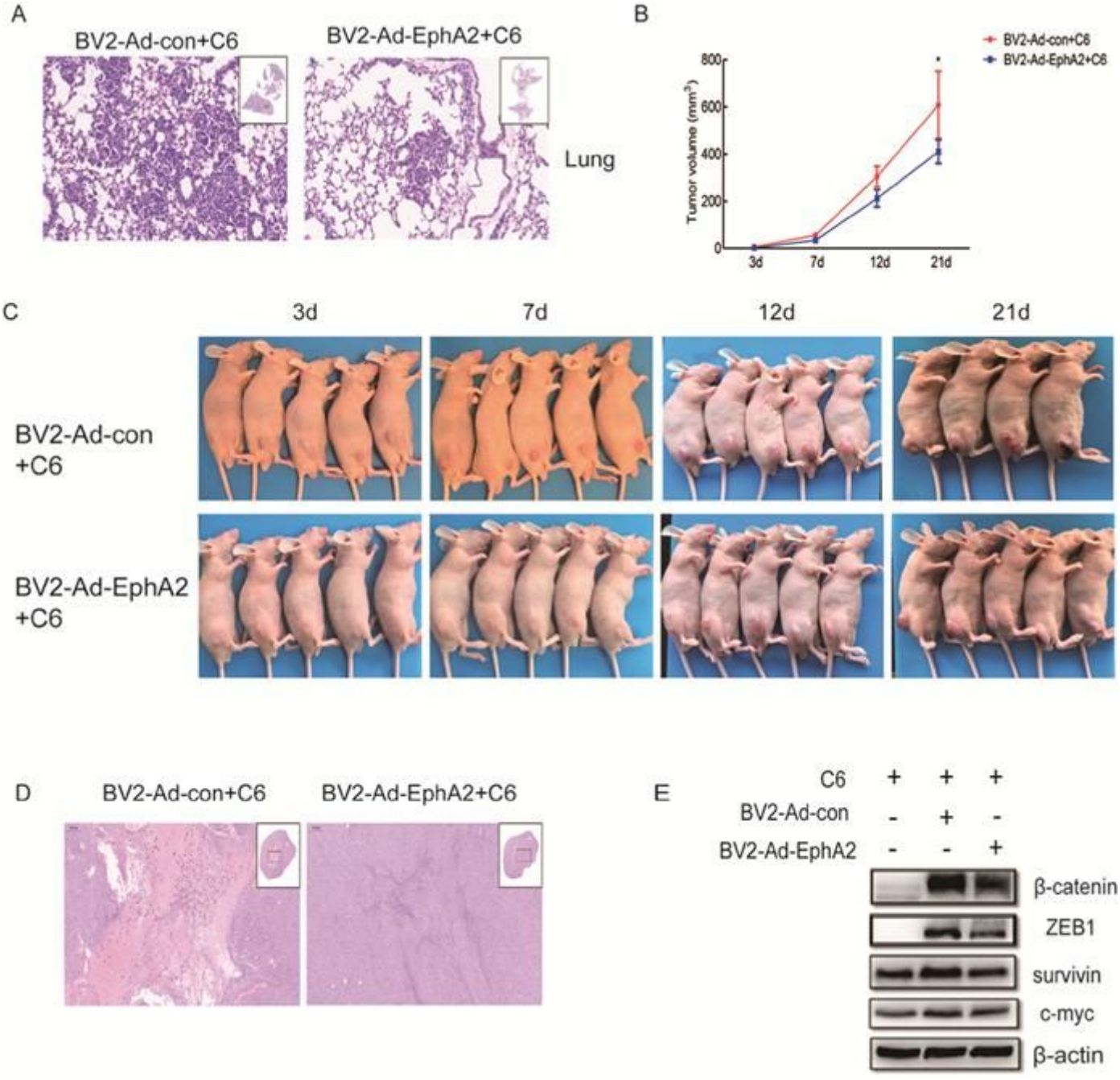

Figure 5

EphA2-mediated M1-like polarization of BV2 inhibited GBM cells proliferation and metastasis in vivo. (A) HE staining was used to verify the lung metastases foci of C6 co-cultured with parental or EphA2 overexpression BV2 cells. Magnification: × 4 and × 20. (B) Nude mice were injected subcutaneously with 1 × 106 C6 cells co-cultured with parental or EphA2 overexpression BV2 cells. Tumor volume was calculated for 3 weeks. (C) Representative photographs of tumor burden mice at the indicated time (3, 7, 12, 21d). (D) HE staining imaging of the necrosis area of subcutaneous tumor tissues at day 21 day after C6 injection. Magnification: × 20. (E) Western blot analysis of the protein expression level of ZEB1, β-catenin, survivin, and c-myc in the isolated tumor tissues. β-actin was detected as a loading control. Experiments were repeated three times, and the data are expressed as the mean ± SEM. * p< 0.05, ** p< 0.01, *** p< 0.001 vs. control group. Statistical analysis was performed using Student's t-test.

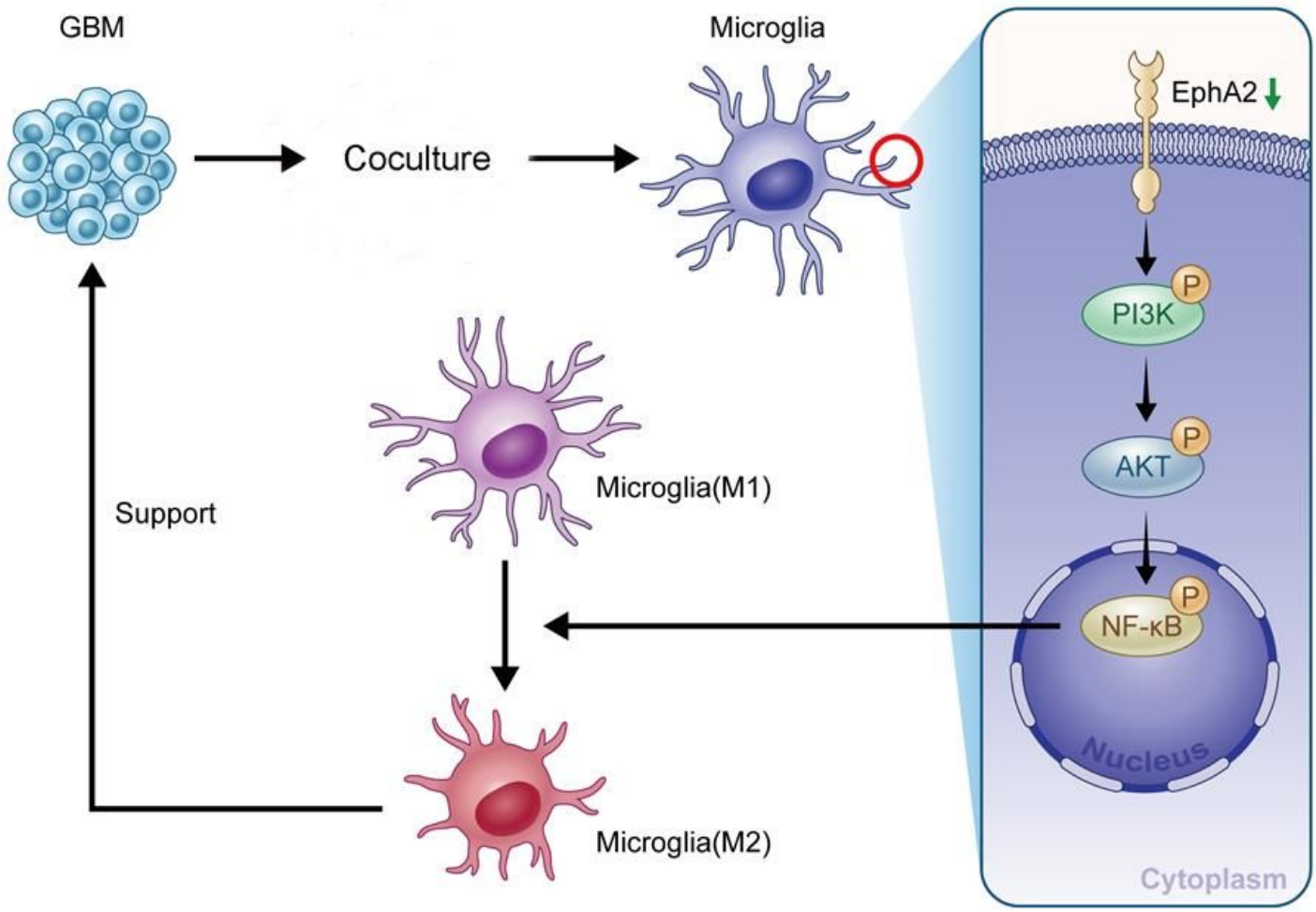

Figure 6

Schematic representation of EphA2-mediated M1-like polarization of microglia in GMB metastasis.

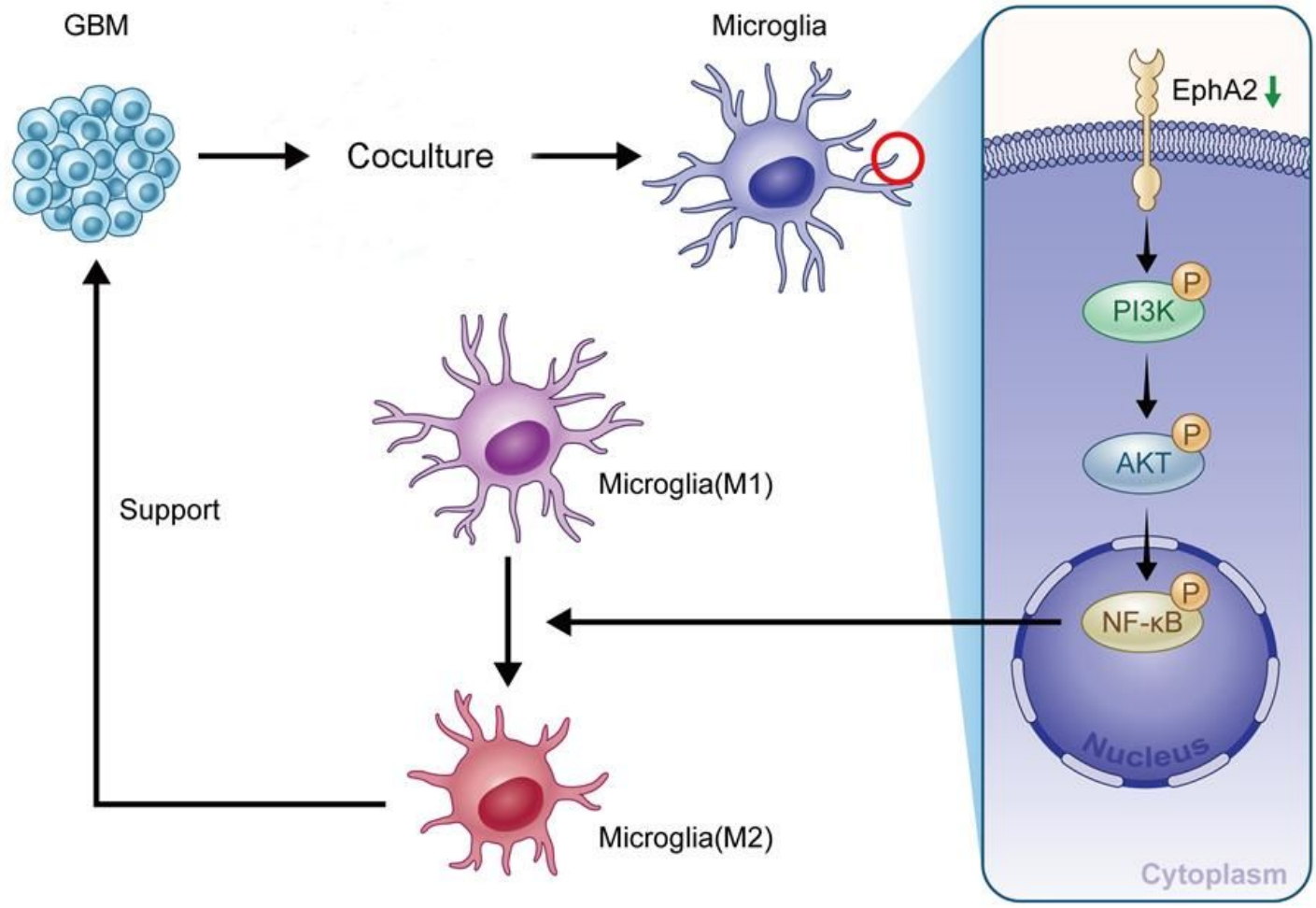

Figure 6

Schematic representation of EphA2-mediated M1-like polarization of microglia in GMB metastasis.

Supplementary Files

This is a list of supplementary files associated with this preprint. Click to download.

- s2.tif
- s2.tif
- S1.tif
- S1.tif
- FigureS1.docx
- FigureS1.docx
- table1.xlsx
- table1.xlsx

- table2.xlsx
- table2.xlsx